Reversible Displacement of Dihydrogen by Carbon Monoxide in Binuclear Platinum Complexes. Characterization of Binuclear Carbonyl Complexes of Platinum(I)

John R. Fisher,[1a] Allan J. Mills,[1a] Steven Sumner,[1a] Michael P. Brown,*[1a] Mary A. Thomson,[1b] Richard J. Puddephatt,*[1b] Aileen A. Frew,[1c] Ljubica Manojlović-Muir,*[1c] and Kenneth W. Muir[1c]

Donnan Laboratories, University of Liverpool, Liverpool L69 3BX, United Kingdom, Department of Chemistry, University of Western Ontario, London, Ontario, Canada N6A 5B7, and Chemistry Department, University of Glasgow, Glasgow G12 8QQ, United Kingdom

Received April 28, 1982

The complex ion $[Pt_2H_2(\mu\text{-}H)(\mu\text{-}dppm)_2]^+$ (I), dppm = $Ph_2PCH_2PPh_2$, reacts reversibly with carbon monoxide to give dihydrogen and a new hydridodiplatinum(I) complex cation, $[Pt_2H(CO)(\mu\text{-}dppm)_2]^+$ (II), which is structurally characterized by its IR and ^1H and $^{31}P\{^1H\}$ NMR spectra. II reacts with PMe_2Ph to give $[Pt_2H(PMe_2Ph)(\mu\text{-}dppm)_2]^+$ and CO and with MeSH to give $[Pt_2H_2(\mu\text{-}SMe)(\mu\text{-}dppm)_2]^+$ and CO. I is formed by reaction of $[Pt_2(CO)_2(\mu\text{-}dppm)_2]^{2+}$ with excess H_2, and reaction of $[Pt_2H_2(\mu\text{-}Cl)(\mu\text{-}dppm)_2]^+$ with CO gives $[Pt_2Cl(CO)(\mu\text{-}dppm)_2]^+$, thus establishing the generality of H_2 for CO displacement reactions in diplatinum complexes. Complex I acts as a homogeneous catalyst for the water gas shift reaction at 100 °C in aqueous methanol, and model reactions indicate that a mechanism involving some of the binuclear intermediates and reactions described above is reasonable. The crystal structure of $[Pt_2(CO)_2(\mu\text{-}dppm)_2][PF_6]_2$ was determined by the heavy-atom method and refined by full-matrix least squares to $R = 0.061$ and $R_w = 0.079$, using 5525 diffractometric X-ray intensities with $I > 3\sigma(I)$. Crystals are monoclinic of space group $P2_1/c$ with $a = 17.298$ (5) Å, $b = 18.913$ (7) Å, $c = 18.884$ (4) Å, $\beta = 98.63$ (2)°, and $Z = 4$. The structure of the cation contains two Pt–CO fragments bridged by two dppm ligands and linked directly by a Pt–Pt σ bond of 2.642 (1) Å. The metal–ligand bond lengths are Pt–C = 1.92 (2) and 1.95 (2) Å and Pt–P = 2.302 (4)–2.340 (4) Å. Variations in the Pt–P distances are likely to arise from steric effects.

Introduction

Reactions in which dihydrogen reversibly displaces coordinated carbon monoxide in transition-metal complexes are rare. Two examples are shown in eq 1 and 2.[2,3]

$$[Ir(CO)_3(PPh_3)_2] + H_2 \rightleftharpoons [IrH_2(CO)_2(PPh_3)_2] + CO \quad (1)$$

$$[Os_3(CO)_{12}] + H_2 \rightleftharpoons [Os_3H_2(CO)_{10}] + 2CO \quad (2)$$

In this paper we report binuclear platinum(I) carbonyl complexes in which a carbonyl ligand can be displaced reversibly by dihydrogen. To the best of our knowledge, no binuclear complex having this property was known prior to our preliminary communication on this topic.[4] We also report other reactions in which dihydrogen or carbon monoxide is displaced from diplatinum complexes, some preliminary observations involving catalysis of the water gas shift reaction by a binuclear hydridoplatinum complex and the structure of the dication $[Pt_2(CO)_2(\mu\text{-}dppm)_2]^{2+}$.

Results and Discussion

Some of the new chemical reactions are summarized in Scheme I. Reaction between carbon monoxide and the binuclear complex[5] $[Pt_2H_2(\mu\text{-}H)(\mu\text{-}dppm)_2]^+X^-$, dppm = $Ph_2PCH_2PPh_2$ (Ia, X = PF_6; Ib, X = BPh_4), gives the hydridocarbonyldiplatinum(I) complex $[Pt_2H(CO)(\mu\text{-}dppm)_2]^+X^-$ (IIa, X = PF_6; IIb, X = BPh_4) together with 1 M proportion of dihydrogen. This is an example of a binuclear reductive elimination reaction in which dihydrogen is eliminated, and the formal oxidation state of each platinum center decreases from +II to +I.[6] The reaction proceeds smoothly in dichloromethane solution at room temperature and, in the presence of excess carbon monoxide at 1 atm pressure, is complete in 48 h. The complex IIa is a yellow, air-stable solid that is very soluble in dichloromethane, acetone, and tetrahydrofuran and slightly soluble in methanol and hot benzene. These solutions, which are initially yellow-orange, darken to red and then to brown-gray unless kept under an atmosphere of carbon monoxide.

Of particular interest is the observation that the displacement of H_2 from Ia by CO is easily reversible. Thus treatment of IIa with excess hydrogen gave Ia in good yield, although slight decomposition giving a dark-colored impurity occurred. This is an example of a binuclear oxidative addition reaction, in the sense that the oxidation states of two platinum atoms are increased by one in the overall reaction. The primary oxidative addition may well occur at a single metal center, however. The reaction of IIa with hydrogen occurred at about the same rate as the reaction of Ia with carbon monoxide.

The carbonyl ligand in IIa is labile and is easily displaced by a tertiary phosphine ligand to give $[Pt_2H(PMe_2Ph)(\mu\text{-}dppm)_2][PF_6]$ (complex III, Scheme I). Complex III has been characterized previously[6,7] and differs from IIa in being unreactive toward dihydrogen. The reaction of IIa with methanethiol to give IV, Scheme I, is another example of a binuclear oxidative addition reaction, and it is possible that the first step involves displacement of CO by MeSH in IIa.[8]

(1) (a) University of Liverpool. (b) University of Western Ontario. (c) University of Glasgow.

(2) Church, M. J.; Mays, M. J.; Simpson, R. N. F.; Stefanini, F. P. *J. Chem. Soc. A* **1970**, 2909. Mays, M. J.; Simpson, R. N. F.; Stefanini, F. P. *Ibid.* **1970**, 3000.

(3) Knox, S. A. R.; Koepke, J. W.; Andrews, M. A.; Kaesz, H. D. *J. Am. Chem. Soc.* **1975**, *97*, 3942. Deeming, A. J.; Hasso, S. *J. Organomet. Chem.* **1979**, *179*, C13.

(4) Brown, M. P.; Fisher, J. R.; Mills, A. J.; Puddephatt, R. J.; Thomson, M. A. *Inorg. Chim. Acta* **1980**, *44*, L271.

(5) Brown, M. P.; Puddephatt, R. J.; Rashidi, M.; Seddon, K. R. *J. Chem. Soc.*, Dalton *Trans.* **1978**, 516.

(6) Brown, M. P.; Fisher, J. R.; Manojlović-Muir, Lj.; Muir, K. W.; Puddephatt, R. J.; Thomson, M. A.; Seddon, K. R. *J. Chem. Soc., Chem. Commun.* **1979**, 931.

(7) Brown, M. P.; Fisher, J. R.; Hill, R. H.; Puddephatt, R. J.; Seddon, K. R. *Inorg. Chem.* **1981**, *20*, 3516.

0276-7333/82/2301-1421$01.25/0

Scheme I

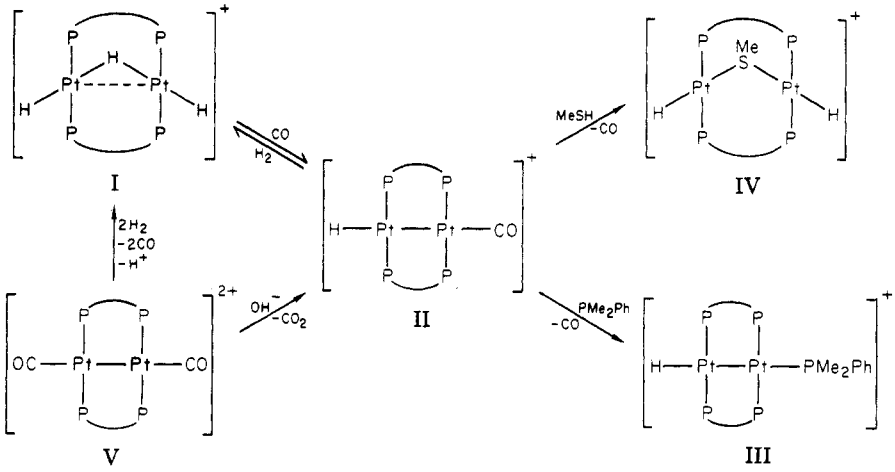

Although only one truly reversible reaction has been discovered, it appears that displacement of H_2 by CO and the reverse may be general reactions in these diplatinum complexes and at least one further example of each has been established. Thus reaction of the diplatinum(I) dication[9] $[Pt_2(CO)_2(\mu\text{-dppm})_2]^{2+}$ (V) with H_2 occurs as shown in eq 3.

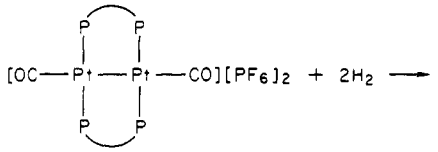

$$Ia + 2CO + H[PF_6] \quad (3)$$

It is likely that IIa is an intermediate in this reaction but it was not identified. Although IIa reacts readily with dihydrogen, the similar chloro carbonyl complex[10] $[Pt_2Cl(CO)(\mu\text{-dppm})_2][PF_6]$ (VI) failed to react with dihydrogen at room temperature. This difference in reactivity may be due to the strong σ-donor hydrido ligand in IIa increasing the electron density in the Pt–Pt bond and so enhancing reactivity to oxidative addition compared to VI. Complex VI can be formed by reaction of $[Pt_2H_2(\mu\text{-Cl})(\mu\text{-dppm})_2][PF_6]$[5] with carbon monoxide according to eq 4. The mechanism here is clearly complex

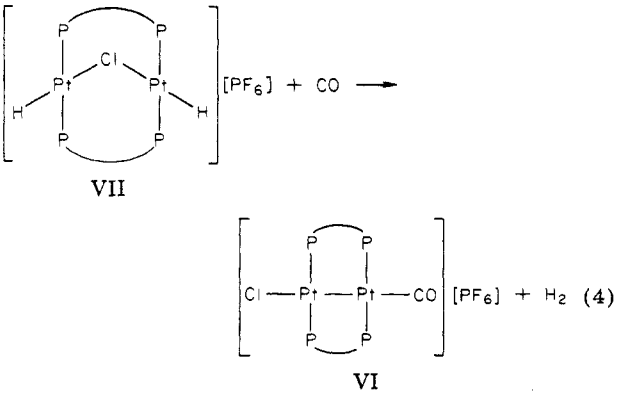

$$[PF_6] + H_2 \quad (4)$$

since the μ-Cl ligand in VII becomes a terminal ligand in VI, while the hydride ligands in VII are well separated and presumably must move into close proximity before reductive elimination of H_2 is possible.

Scheme II. A Possible Mechanism for Catalysis of the Water Gas Shift Reaction

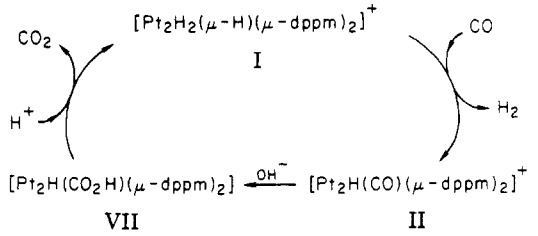

The ease with which the reaction of Ia with CO occurred suggested that I or II might act as catalysts for the water gas shift reaction.[11] Thus it is well-known that cationic carbonyl complexes can react with water to give a metal hydride and carbon dioxide (e.g., eq 5)[12,13]

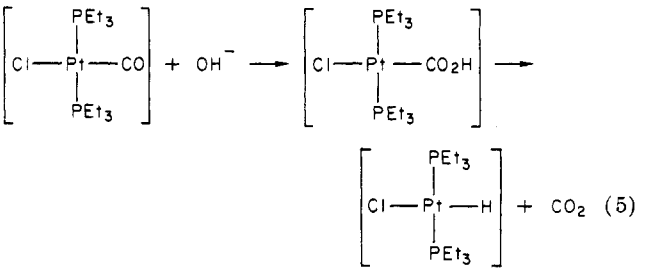

$$CO_2 + H_2 \quad (5)$$

By analogy with this known chemistry, the water gas shift could be expected to occur as shown in Scheme II. Our attempts to demonstrate this mechanism using model reactions have been unsuccessful. Thus reaction of IIa with water does not occur at room temperature even in the presence of base, and at higher temperatures general decomposition of II occurred. The carbonyl ligand in II is thus less susceptible to nucleophilic attack than that in *trans*-$[PtCl(CO)(PEt_3)_2]^+$, possibly because the positive charge in II is dispersed over a larger molecule leaving less positive charge on the carbonyl carbon. However, the dication V does react with OH^- (Scheme I), and the catalytic reaction does occur readily. Thus at 100 °C under pressure of carbon monoxide (50 psi) in aqueous methanol, catalysis using Ia gave equal amounts of H_2 and CO_2 with

(8) Brown, M. P.; Fisher, J. R.; Puddephatt, R. J.; Seddon, K. R. *Inorg. Chem.* **1979**, *18*, 2808.
(9) Brown, M. P.; Franklin, S. J.; Puddephatt, R. J.; Thomson, M. A.; Seddon, K. R. *J. Organomet. Chem.* **1979**, *178*, 281.
(10) Brown, M. P.; Puddephatt, R. J.; Rashidi, M.; Seddon, K. R. *J. Chem. Soc., Dalton Trans.* **1978**, 1540.
(11) Yoshida, T.; Ueda, Y.; Otsuka, S. *J. Am. Chem. Soc.* **1978**, *100*, 3941. Baker, E. C.; Hendrikson, D. E.; Eisenberg, R. *J. Am. Chem. Soc.* **1980**, *102*, 1020. King, A. D., Jr.,; King, R. B.; Yang, D. B. *Ibid.* **1980**, *102*, 1028. Laine, R. M.; Rinker, R. G.; Ford, P. C. *Ibid.* **1977**, *99*, 252.
(12) Clark, H. C.; Jacobs, W. J. *Inorg. Chem.* **1970**, *9*, 1229.
(13) Catellani, M.; Halpern, J. *Inorg. Chem.* **1980**, *19*, 566.

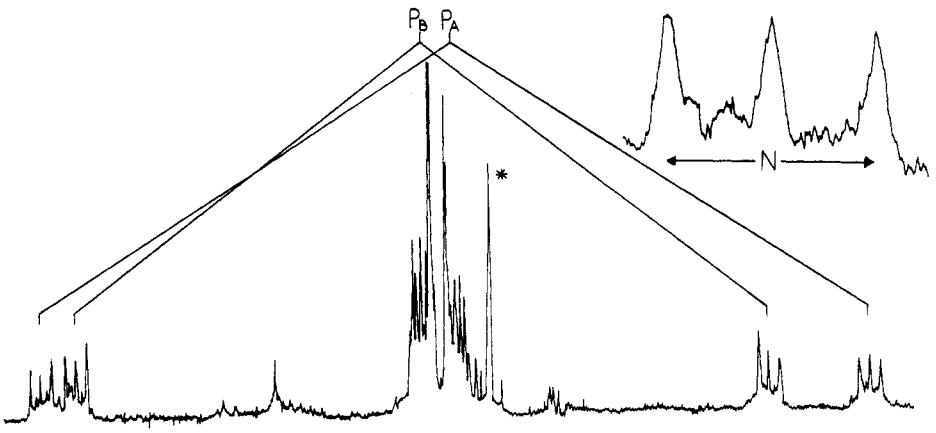

Figure 1. The $^{31}P\{^1H\}$ NMR spectrum (40.5 MHz) of complex IIa in CH_2Cl_2. The peak marked asterisk is the reference $(MeO)_3PO$.

a turnover rate of ca. 3.5 (mol of H_2 or CO_2)/(mol of catalyst) (h). Probably, the excess carbon monoxide prevents general decomposition of IIa initiated by dissociation of the labile carbonyl ligand. A detailed study of this process is being carried out, and it is hoped to consider the mechanism in greater detail at a later date. Kubiak and Eisenberg have recently reported a somewhat analogous catalysis of the water gas shift reaction by using $[Rh_2(\mu\text{-}H)(\mu\text{-}CO)(CO)_2(\mu\text{-dppm})_2]^+$ as catalyst.[14]

Characterization of the Cation $[Pt_2H(CO)(\mu\text{-dppm})_2]^+$. The molecular formula of the complex is established from the analytical data and particularly from the stoichiometry of the formation of IIa from I and carbon monoxide and the reverse reaction. The problem is therefore to distinguish between the possible structures, of which A and B are most probable, a priori (P⌒P = diphosphine).

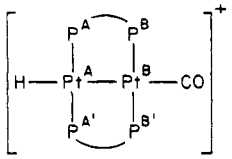

A

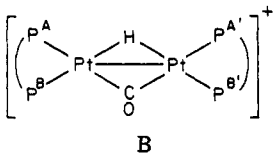

B

A complex ion of structure B has been discovered recently, with P⌒P = 1,2-bis(diphenylphosphino)ethane, dppe, and was characterized by X-ray crystallography.[15] The infrared spectrum of $[Pt_2(\mu\text{-}H)(\mu\text{-}CO)(dppe)_2][BF_4]$ contained a band at 1730 cm^{-1} due to the μ-CO group. In contrast complex IIa has ν(CO) 2040 cm^{-1}, clearly indicating a terminal carbonyl group as expected for structure A.

The presence of a terminal hydride ligand in IIa is demonstrated by the ^1H NMR spectrum in the platinum hydride region. The resonance appears as a multiplet due to coupling with ^{31}P atoms [δ(PtH) −6.73 (^2J(PH) = 11 Hz, ^3J(PH) = 6 Hz)] with two sets of one-fourth intensity satellites due to coupling with the near and far ^{195}Pt atoms [^1J(PtH) = 990 Hz, ^2J(PtH) = 61 Hz]. A complex with structure B would show only a ^1J(PtH) coupling, and the resonance would appear as a 1:8:18:8:1 quintet with lines separated by one-half ^1J(PtH).[5] The coupling constants involving the platinum hydride are very similar to corresponding values for complexes $[Pt_2H(L)(\mu\text{-dppm})_2]^+$, L = tertiary phosphine, one of which has been structurally characterized by X-ray methods, and this further supports the structure A.[6,7] The infrared spectrum of complex IIa contains no resolved band due to ν(Pt–H) presumably because it is obscured by the relatively broad and intense ν(CO) band at 2040 cm^{-1}. The spectrum of complex IIB is more clearly resolved and shows two bands in this region, an intense band at 2054 cm^{-1}, assigned to ν(CO), and a weaker band at 2024 cm^{-1}. It seems probable that this weaker band is due to ν(Pt–H).

The presence of μ-dppm groups is indicated by both the ^1H and $^{31}P\{^1H\}$ NMR spectra. In the ^1H NMR spectrum the CH_2P_2 protons gave a singlet at δ 5.28 with two sets of one-fourth intensity satellites due to coupling with nonequivalent ^{195}Pt atoms (Pt^A and Pt^B) with ^3J(PtH) = 75 and 38 Hz. Similar features have been observed in analogous complexes such as III.[6,7] The $^{31}P\{^1H\}$ NMR spectrum of IIa is shown in Figure 1. The spectrum was similar to that found for the complex ion $[Pt_2Cl(CO)(\mu\text{-dppm})_2]^+$, whose ^{31}P NMR spectrum has been discussed previously and whose structure, deduced from the spectroscopic data,[10] has been confirmed by an X-ray structure determination.[16] The central resonance is analyzed as an AA′BB′ spin system (see structure A for labeling scheme), and there are satellites about $\delta(P^A,P^{A'})$ and $\delta(P^B,P^{B'})$ due to isotopmers in which Pt^A or Pt^B is a ^{195}Pt atom ($I = {}^1/_2$, natural abundance 33.8%). The one-bond couplings $^1J(Pt^AP^A)$ = 3355 Hz and $^1J(Pt^BP^B)$ = 2805 Hz are easily identified (Figure 1), and the midpoints between the satellites give accurate values of $\delta(P^A,P^{A'})$ 3.60 and $\delta(P^B,P^{B'})$ 6.81. From the satellites, a doublet splitting $N = J(P^AP^B) + J(P^AP^{B'})$ = 86 Hz is easily identified, but a second expected splitting $L = J(P^AP^B) - J(P^AP^{B'})$ is not observed and is clearly too small to be resolved. Hence $J(P^AP^B) \approx J(P^AP^{B'}) \approx 43$ Hz. The central AA′BB′ resonance was then simulated by using the computer program LAOCN3 and gave accurate values of $J(P^AP^B)$ = 46 Hz and $J(P^AP^{B'})$ = 40 Hz. In the simulation $J(P^AP^{A'})$ was necessarily large, and a value of 500 Hz was found satisfactory, although the calculated spectrum was insensitive to small changes in this coupling and it could not be refined. Such a value is expected for structure A with μ-dppm groups but not for structure B in which a low value of $J(P^AP^{A'})$ would be expected. Finally the long-range couplings $^2J(Pt^AP^B)$ = 62 Hz and $^2J(Pt^BP^A)$ = 82 Hz were identified (these satellites overlap with the main AA′BB′ spectrum and are not easily found). Resonances due to isotopomers in which both Pt^A and Pt^B are ^{195}Pt centers could not be found and so the coupling $^1J(Pt^APt^B)$ was not identified.

The Structure of $[Pt_2(CO)_2(\mu\text{-dppm})_2][PF_6]_2$. In the crystal structure the asymmetric unit contains one cation,

(14) Kubiak, C. P.; Eisenberg, R. *J. Am. Chem. Soc.* **1980**, *102*, 3637.
(15) Minghetti, G.; Bandini, A. L.; Banditelli, G.; Bonati, F. *J. Organomet. Chem.* **1979**, *179*, C13.
(16) Manojlović-Muir, Lj.; Muir, K. W.; Solomun, T. *J. Organomet. Chem.* **1979**, *179*, 479.

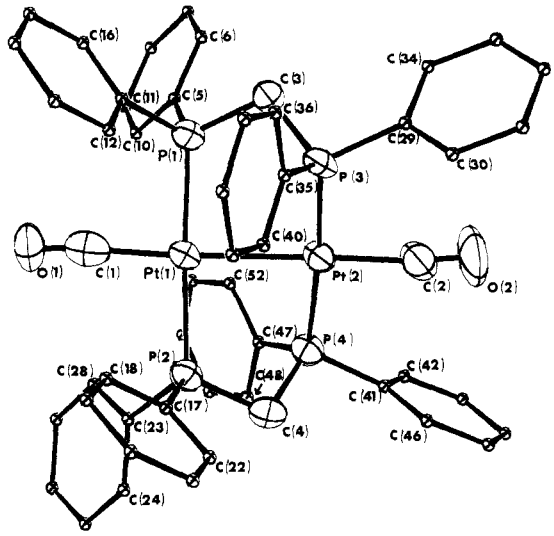

Figure 2. The structure of the $[Pt_2(CO)_2(\mu\text{-dppm})_2]^{2+}$ cation. The vibrational ellipsoids of Pt, P, O, and C(1)–C(4) atoms display 50% probability. For clarity, the phenyl ring carbon atoms are represented by spheres of arbitrary size; in each phenyl ring only three C atoms are labeled and they indicate the direction of the progressive sequence C(n), C(n + 1), ..., C(n + 5).

two anions, and a highly disordered solvent molecule whose identity was not established by the diffraction analysis described here. The cations and anions are well separated from each other, except for two short F···H contacts which could be indicative of weak hydrogen bonding [F(10)···H(3^I) = 2.13 Å and F(10)···H(46^I) = 2.22 Å, where the superscript I refers to hydrogen atoms[17] at $1 - x$, $^1/_2 + y$, $^1/_2 - z$].

The structure of the $[P(6)F_6]^-$ anion is unexceptional. The P(6)–F bond lengths, which range from 1.55 (1) to 1.58 (1) Å, agree to within experimental error and the F–P(6)–F bond angles are all within 4° from 90 or 180° (Table I). In contrast, the $[P(5)F_6]^-$ anion is likely to be disordered, as suggested by the exceptionally large vibrational parameters of its atoms (Table IV) and by the appearance of the final difference synthesis. Consequently, the geometry of the $[P(5)F_6]^-$ ion is determined poorly compared with the rest of the structure (Table I), the P(5)–F(3) bond length [1.40 (3) Å] being particularly anomalous.

The structure of the cation, shown in Figure 2, comprises two PtCO fragments bridged by two dppm ligands and linked directly by a covalent Pt–Pt bond. The coordination geometry around each metal atom is square planar with small tetrahedral distortions. These distortions are evident from the bond angles subtended at Pt(1) and Pt(2) (Table I) and from the displacements of the atoms from the Pt_2P_2C coordination planes, which do not exceed ±0.06 Å. The two dppm ligands exhibit similar conformations, and the structure of the cation approximates to C_2 symmetry, the diad axis coinciding with the roughly linear OC–Pt–Pt–CO fragment.

Hence, the $[Pt_2(CO)_2(\mu\text{-dppm})_2]^{2+}$ cation adopts a solid-state structure that is in agreement with that deduced from its IR and solution ^1H and ^{31}P NMR spectra.[9] Similar structures have previously been found in the complexes $[Pt_2Cl_2(\mu\text{-dppm})_2]$, $[Pt_2Cl(CO)(\mu\text{-dppm})_2]^+$, and $[Pt_2H(dppm)(\mu\text{-dppm})_2]$.[+6,16,18] This structural type can thus be considered characteristic of the binuclear platinum(I) complexes $[Pt_2XY(dppm)_2]^{n+}$, where n = 0, 1, or 2 and X and Y are one- or two-electron-donor ligands.

The conformations of the dppm ligands around the P–C (sp^3), P–Pt, and Pt–Pt bonds are described by the torsion angles listed in Table I. The Pt_2P_2C metallocycles show similar conformations which can be described as intermediate between half-chair and envelope: the atoms C(3) and P(3) are displaced by 0.64 (1) and 1.457 (4) Å, respectively, from the $Pt_2P(1)$ plane and the atoms C(4) and P(4) are 0.50 (1) and 1.499 (4) Å away from the $Pt_2P(2)$ plane. The cation therefore adopts the usual twisted configuration,[6,16,18] in which the metal atom coordination planes are mutually rotated about the Pt–Pt bond to give a dihedral angle of 40.0°. Such a configuration leads to sterically different environments of the two axial carbonyl ligands and also of the two coordinatively unsaturated metal centers, as is evident from Figure 2. The C(1) atom is surrounded by four phenyl groups with which its shortest contacts are the following: C(1)···H(10) = 2.77 Å, C(1)···H(18) = 2.59 Å, and C(1)···H(28) = 2.61 Å. In the proximity of C(2) there are only two phenyl groups and none of the C(2)···H separations is shorter than the van der Waals distance of 2.90 Å. The Pt(1) atom is shielded by a cage of six phenyl rings, while the Pt(2) atom is in a much more exposed environment. Thus, if the solid-state configuration of the $[Pt_2(CO)_2(\mu\text{-dppm})_2]^{2+}$ is retained in solution, it is possible that one metal atom of this binuclear species is more easily attacked in the reactions with small molecules described earlier.

The CO group attached to the Pt(1) atom can be considered linear [Pt(1)–C(1)–O(1) = 177.8 (15)°] and that attached to Pt(2) slightly bent [Pt(2)–C(2)–O(2) = 172.2 (18)°]. The Pt–C [1.92 (2) and 1.95 (2) Å] and C–O [1.14 (2) and 1.08 (2) Å] distances are in agreement with those [1.89 (2) and 1.15 (3) Å] previously found in $[Pt_2Cl(CO)(\mu\text{-dppm})_2][PF_6]$.[16]

In the dppm ligands, the Pt(2)–P–C(sp^3) angles [101.6 (5) and 106.6 (5)°] are unusually small compared with the Pt(1)–P–C(sp^3) angles [113.7 (5) and 114.8 (4)°], while the P–C(sp^3)–P angles [106.6 (7) and 108.9 (7)°] remain close to the tetrahedral value. The bond lengths and the other bond angles are the following: P–C(sp^3) = 1.818 (14)–1.829 (14) Å, P–C(sp^2) = 1.793 (10)–1.823 (10) Å, C–P–C = 102.8 (6)–108.2 (6)°, and Pt–P–C(sp^2) = 109.5 (4)–119.3 (4)° (Table I). The Pt(2)–P distances [2.302 (4) and 2.303 (4) Å] are equal to the Pt–P (cis to CO) distances [2.303 (5) and 2.308 (5) Å] in the closely related complex $[Pt_2Cl(CO)(\mu\text{-dppm})_2]^+$, where the carbonyl ligand is attached to the platinum atom in the sterically more open environment.[16] The Pt(1)–P bonds [2.334 (4) and 2.340 (4) Å], however, are ca. 0.035 Å longer than the Pt(2)–P bonds, and their lengthening can be attributed to steric effects. A contraction of these bonds would result in steric crowding around the Pt(1)–CO fragment more severe than that described above.

The Pt(1)–Pt(2) separation [2.642 (1) Å], ca. 0.3 Å shorter than the P···P distances in the dppm ligands [2.916 (6) and 2.969 (6) Å], indicates a bonding interaction and lies within the range of Pt–Pt bond lengths observed in other platinum(I) binuclear species [2.531 (1)–2.769 (1) Å].[6,16,18,19] In the complexes $[Pt_2Cl(CO)(\mu\text{-dppm})_2]^+$, $[Pt_2(CO)_2(\mu\text{-dppm})_2]^{2+}$, $[Pt_2Cl_2(\mu\text{-dppm})_2]$, and $[Pt_2H(dppm)(\mu\text{-dppm})_2]^+$ the Pt–Pt distances are 2.620 (1), 2.642 (1), 2.651 (1), and 2.769 (1) Å, respectively. This sequence appears to reflect mainly the trans-influencing capabilities

(17) The atoms H(1) and H(2) are bonded to C(3) and H(3) and H(4) to C(4); the phenyl group hydrogens are labeled by the same numbers as the carbon atoms to which they are attached.

(18) Manojlović-Muir, Lj.; Muir, K. W.; Solomun, T. *Acta Crystallogr.* **1979**, B35, 1237.

(19) Boag, N. M.; Browning, J.; Crocker, C.; Goggin, P. L.; Goodfellow, R. J.; Murray, M.; Spencer, J. L. *J. Chem. Res., Synop.* **1978**, 228; *J. Chem. Res., Miniprint* **1978**, 2962.

Table I. Selected Interatomic Distances (Å) and Angles (Deg) in $[Pt_2(CO)_2(\mu\text{-dppm})_2][PF_6]_2$

Bond Distances

Cation

Pt(1)-Pt(2)	2.642 (1)	P(2)-C(23)	1.816 (9)
Pt(1)-P(1)	2.334 (4)	P(3)-C(29)	1.796 (11)
Pt(1)-P(2)	2.340 (4)	P(3)-C(35)	1.823 (10)
Pt(2)-P(3)	2.303 (4)	P(4)-C(41)	1.809 (9)
Pt(2)-P(4)	2.302 (4)	P(4)-C(47)	1.793 (10)
Pt(1)-C(1)	1.92 (2)	P(1)···P(3)	2.969 (6)
Pt(2)-C(2)	1.95 (2)	P(2)···P(4)	2.916 (6)
O(1)-C(1)	1.14 (2)	C(1)···P(1)	2.97
O(2)-C(2)	1.08 (2)	C(1)···P(2)	3.14
P(1)-C(3)	1.829 (14)	C(2)···P(3)	3.11
P(2)-C(4)	1.818 (14)	C(2)···P(4)	3.08
P(3)-C(3)	1.821 (14)	C(1)···H(10)[a]	2.77
P(4)-C(4)	1.820 (14)	C(1)···H(18)	2.59
P(1)-C(5)	1.808 (10)	C(1)···H(28)	2.61
P(1)-C(11)	1.810 (10)	Pt(1)···H(52)	2.94
P(2)-C(17)	1.810 (11)		

Anions

P(5)-F(1)	1.53 (2)	P(6)-F(7)	1.58 (2)
P(5)-F(2)	1.56 (2)	P(6)-F(8)	1.57 (2)
P(5)-F(3)	1.40 (3)	P(6)-F(9)	1.55 (2)
P(5)-F(4)	1.51 (3)	P(6)-F(10)	1.55 (2)
P(5)-F(5)	1.56 (2)	P(6)-F(11)	1.57 (2)
P(5)-F(6)	1.52 (3)	P(6)-F(12)	1.57 (2)

Bond Angles

Cation

Pt(2)-Pt(1)-P(1)	89.1 (1)	Pt(1)-Pt(2)-P(3)	88.0 (1)
Pt(2)-Pt(1)-P(2)	88.3 (1)	Pt(1)-Pt(2)-P(4)	86.4 (1)
Pt(2)-Pt(1)-C(1)	177.2 (5)	Pt(1)-Pt(2)-C(2)	178.5 (6)
P(1)-Pt(1)-P(2)	174.6 (1)	P(3)-Pt(2)-P(4)	173.5 (1)
P(1)-Pt(1)-C(1)	88.1 (5)	P(3)-Pt(2)-C(2)	93.4 (6)
P(2)-Pt(1)-C(1)	94.5 (5)	P(4)-Pt(2)-C(2)	92.2 (6)
Pt(1)-C(1)-O(1)	177.8 (15)	Pt(2)-C(2)-O(2)	172.2 (18)
P(1)-C(3)-P(3)	108.9 (7)	P(2)-C(4)-P(4)	106.6 (7)
Pt(1)-P(1)-C(3)	114.8 (4)	Pt(2)-P(3)-C(3)	106.6 (5)
Pt(1)-P(1)-C(5)	116.6 (4)	Pt(2)-P(3)-C(29)	115.5 (4)
Pt(1)-P(1)-C(11)	109.5 (4)	Pt(2)-P(3)-C(35)	117.5 (4)
Pt(1)-P(2)-C(4)	113.7 (5)	Pt(2)-P(4)-C(4)	101.6 (5)
Pt(1)-P(2)-C(17)	110.9 (4)	Pt(2)-P(4)-C(41)	114.0 (4)
Pt(1)-P(2)-C(23)	115.9 (4)	Pt(2)-P(4)-C(47)	119.3 (4)
C(3)-P(1)-C(5)	105.2 (5)	C(3)-P(3)-C(29)	105.6 (6)
C(3)-P(1)-C(11)	104.3 (6)	C(3)-P(3)-C(35)	107.1 (6)
C(5)-P(1)-C(11)	105.4 (5)	C(29)-P(3)-C(35)	103.7 (5)
C(4)-P(2)-C(17)	107.2 (6)	C(4)-P(4)-C(41)	106.6 (6)
C(4)-P(2)-C(23)	102.8 (6)	C(4)-P(4)-C(47)	108.2 (6)
C(17)-P(2)-C(23)	105.6 (5)	C(41)-P(4)-C(47)	106.3 (5)

Anions

cis-F-P-F	84.1 (14)-95.9 (18)
trans-F-P-F	174.2 (17)-179.8 (12)

Torsion Angles (Deg) in the Cation

P(1)-Pt(1)-Pt(2)-P(3)	39.3 (1)	P(2)-Pt(1)-Pt(2)-P(4)	40.7 (1)
Pt(1)-Pt(2)-P(3)-C(3)	−56.4 (5)	Pt(1)-Pt(2)-P(4)-C(4)	−63.4 (5)
Pt(2)-P(3)-C(3)-P(1)	48.7 (7)	Pt(2)-P(4)-C(4)-P(2)	60.4 (7)
P(3)-C(3)-P(1)-Pt(1)	−12.3 (8)	P(4)-C(4)-P(2)-Pt(1)	−23.6 (8)
C(3)-P(1)-Pt(1)-Pt(2)	−22.7 (5)	C(4)-P(2)-Pt(1)-Pt(2)	−17.4 (5)
P(1)-Pt(1)-Pt(2)-P(4)	−144.0 (1)	P(2)-Pt(1)-Pt(2)-P(3)	−135.9 (1)
C(1)-Pt(1)-P(1)-C(5)	−79.5 (6)	C(2)-Pt(2)-P(3)-C(29)	7.3 (7)
C(1)-Pt(1)-P(1)-C(11)	40.0 (6)	C(2)-Pt(2)-P(3)-C(35)	−115.7 (7)
C(1)-Pt(1)-P(2)-C(17)	−75.9 (7)	C(2)-Pt(2)-P(4)-C(41)	1.8 (7)
C(1)-Pt(1)-P(2)-C(23)	44.4 (6)	C(2)-Pt(2)-P(4)-C(47)	−125.2 (7)
P(3)-C(3)-P(1)-C(5)	−141.8 (6)	P(4)-C(4)-P(2)-C(17)	−146.5 (6)
P(3)-C(3)-P(1)-C(11)	107.6 (7)	P(4)-C(4)-P(2)-C(23)	102.4 (7)
P(1)-C(3)-P(3)-C(29)	172.0 (6)	P(2)-C(4)-P(4)-C(41)	180.0 (6)
P(1)-C(3)-P(3)-C(35)	−77.9 (7)	P(2)-C(4)-P(4)-C(47)	−66.0 (8)

[a] The numbering scheme of hydrogen atoms is shown in ref 1.

of the axial CO, Cl^-, dppm, and H^- ligands.

Experimental Section

General techniques and the synthesis of starting materials have been discussed elsewhere.[5,7-10] NMR spectra were recorded by using Perkin-Elmer R12B or Varian XL100 spectrometers. ^{31}P chemical shifts are given with respect to trimethylphosphate reference, positive values indicating downfield shifts.

Investigation of the Stoichiometry of Carbon Monoxide and Hydrogen Production from the Interconversion of

$[Pt_2H_2(\mu\text{-}H)(\mu\text{-}dppm)_2][PF_6]$ and $[Pt_2H(CO)(\mu\text{-}dppm)_2][PF_6]$. (a) Experimental Method. The reaction vessel consisted of a glass tube fitted with a PTFE vacuum stopcock (4-mm bore) and a standard socket (10/19) had an inlet (11-mm i.d.) on the side to receive a serum cap and had a total volume of 37.8 mL. Solid reactant and solvent were conveniently admitted by removing the stopcock plunger and adding them through the stopcock aperture. Carbon monoxide or hydrogen was then admitted by using conventional vacuum line technique, to a total pressure of approximately 1 atm inclusive of the vapor pressure of solvent (dichloromethane). The quantity of reactant gas (approximately a 20-fold excess) was determined at the end of the reaction, due allowance being made for the (small) quantity consumed in the reaction.

The gases were analyzed on a VG Micromass 12 mass spectrometer with the slits set wide (1.016 mm) to give flat-topped peaks. At the end of the reaction period, helium (1.00 mL at a known temperature and pressure) was admitted through the serum cap and used as an internal standard. The gas phase was made homogeneous by shaking the contents of the vessel. A standard volume of the gas was admitted to the mass spectrometer via the PTFE stopcock, a sampling device and a batch inlet system fitted with a porous disk leak. A pressure of 7×10^{-7} torr was produced in the source chamber. For calibration, standard mixtures were made up in a vessel identical with the reaction vessel. A known amount of reactant gas was introduced via the vacuum line. Solvent (1.5 mL) was then added. Standard amounts of the appropriate product gas (0.1–1.0 mL as necessary) and helium (1.00 cm^3) were then introduced via the serum cap. The analyses were based on ratios of peak heights of hydrogen (m/e 2) or carbon monoxide (m/e 28) to that of helium (m/e 4) and a knowledge of the amount of helium added. A linear relationship between peak height and concentration ratios was assumed only over a narrow range. Correction was made for background intensities. Reproducibility was generally better than ±2%, and accuracy was estimated to be ±4%.

(b) Yield of Hydrogen from Reaction of $[Pt_2H_2(\mu\text{-}H)(\mu\text{-}dppm)_2][PF_6]$ with Carbon Monoxide. A solution of $[Pt_2H_2(\mu\text{-}H)(\mu\text{-}dppm)_2][PF_6]$ (0.0514 g, 0.0393 mmol) in dichloromethane (1.5 mL) was thus treated with carbon monoxide (17.2 mL at STP, 0.769 mmol) for a 24-h period at 20 °C with gentle agitation. This produced 0.0359 mmol of hydrogen (91.3% yield). The permanent gases were then completely pumped away at −196 °C, and the solution was degassed. A second similar treatment with carbon monoxide (18.9 mL at STP, 0.842 mmol) for 24 h gave a further 0.0033 mmol of hydrogen (8.4% yield). The total yield of hydrogen (0.0392 mmol) was therefore 99.7% of 1 M proportion. The IR spectrum of the residual solid product, after removal of solvent, was identical with that of $[Pt_2H(CO)(\mu\text{-}dppm)_2][PF_6]$ products in other experiments (see below).

(c) Yield of Carbon Monoxide from Reaction of $[Pt_2H(CO)(\mu\text{-}dppm)_2][PF_6]$ with Hydrogen. In a similar manner, $[Pt_2H(CO)(\mu\text{-}dppm)_2][PF_6]$ (0.0507 g, 0.0380 mmol) in dichloromethane (1.5 mL) was treated with hydrogen (20.5 mL at STP, 0.916 mmol) for 24 h at 20 °C with gentle agitation. This produced 0.0236 mmol of carbon monoxide (62.1% yield). Two further similar treatments with hydrogen (22.8 mL at STP, 1.02 mmol, and 25.1 mL at STP, 1.12 mmol) were carried out and gave further quantities of carbon monoxide (0.0110 mmol 29.1%, and 0.0014 mmol, 3.8%, respectively). The total yield of carbon monoxide (0.0360 mmol) was therefore 95.0% of 1 M proportion. The solid product from this experiment obtained by complete evaporation of the solvent consisted of white crystals of $[Pt_2H_2(\mu\text{-}H)(\mu\text{-}dppm)_2][PF_6]$ contaminated by a small amount of dark brown oily material.

Preparation of $[Pt_2H(CO)(\mu\text{-}dppm)_2][PF_6]$. (a) In a typical experiment, $[Pt_2H_2(\mu\text{-}H)(\mu\text{-}dppm)_2][PF_6]$ (0.4 g) in dichloromethane (5 mL) was placed in a flask (50 mL) fitted with a serum cap. The air was completely displaced by bubbling carbon monoxide through the flask for ~10 min, and it was then kept in the dark at room temperature for ~24 h. During this time, the almost colourless solution became yellow-orange. Carbon monoxide was then again bubbled through for ~10 min and the reaction allowed to continue for a further 24 h. The product was obtained in essentially quantitative yield as an amorphous yellow powder by completely evaporating the solvent in a stream of carbon monoxide. In other experiments it was recovered in crystalline form (in yields of 75%) by partial evaporation of the solvent followed by careful addition of methanol. Once crystallized, the yellow complex could be filtered off in the air without decomposition. Anal. Calcd for $[Pt_2H(CO)(\mu\text{-}dppm)_2][PF_6]$: C, 46.0; H, 3.4; F, 8.6; P, 11.6. Found: C, 45.8; H, 3.5; F, 8.7; P, 11.5. Infrared spectra of the amorphous and crystalline products were similar except that the spectrum of the latter was better resolved. A strong band at 2040 cm^{-1} is assigned to ν(CO), and this band presumably obscures the weaker ν(Pt–H) band at about the same frequency.

When solutions of the complex are handled in the air, some decomposition occurs as evidenced by the color changing from yellow-orange to red and then to brown. This also occurs under nitrogen but not under carbon monoxide, and thus it appears that decomposition occurs via loss of CO. The solid is much more stable in the air although, if it is to be kept for some weeks, it is necessary to store it under carbon monoxide.

(b) A solution of sodium hydroxide (0.056 g, 0.14 mmol) in methanol (0.5 mL) was added to a stirred solution of $[Pt_2(CO)_2(\mu\text{-}dppm)_2][PF_6]_2$ 0.078 g, 0.05 mmol) in methanol (10 mL). The solution immediately darkened in color. After 0.5 h, the solvent was removed in a stream of N_2 and the orange residue was washed with water to yield IIa (0.064 g, 94%), identified by comparison of the IR spectrum with that an authentic sample prepared as in a above. Carbon dioxide was detected qualitatively by GC as a product of reaction.

Preparation of $[Pt_2H_2(\mu\text{-}H)(\mu\text{-}dppm)_2][BPh_4]$. Crude $[Pt_2H_2(\mu\text{-}H)(\mu\text{-}dppm)_2]Cl$ (0.52 g, 0.43 mmol), prepared as previously described, was dissolved in boiling methanol (55 mL) and the hot solution filtered. The filtrate was allowed to collect in a methanolic solution of sodium tetraphenylborate (0.30 g, 0.88 mmol in 5 mL) when the desired product (0.38 g, 59%) crystallized immediately as a white solid.

Preparation of $[Pt_2H(CO)(\mu\text{-}dppm)_2][BPh_4]$. This complex was prepared in a similar way by treating the tetraphenylborate $[Pt_2H_2(\mu\text{-}H)(\mu\text{-}dppm)_2][BPh_4]$ (0.62 g, 0.42 mmol) in dichloromethane (7 mL) with carbon monoxide over a 48-h period. At intervals of ~12 h the flask was flushed with fresh carbon monoxide. The solvent was completely removed to give initially a sticky solid that dried to a powder in vacuo. This was then crystallized from dichloromethane/methanol to yield the pure product (0.58 g, 0.38 mmol, 92%) as yellow crystals. Anal. Calcd for $[Pt_2H(CO)(\mu\text{-}dppm)_2][BPh_4]$: C, 59.8; H, 4.4; P, 8.2. Found: C, 59.5; H, 4.4; P, 8.1. This salt gives a better resolved IR spectrum than the PF_6^- salt, and bands at 2056 and 2024 cm^{-1} are clearly resolved and assigned to ν(CO) and ν(Pt–H), respectively.

Reaction of $[Pt_2H(CO)(\mu\text{-}dppm)_2][PF_6]$ with Hydrogen. A sample of $[Pt_2H(CO)(\mu\text{-}dppm)_2][PF_6]$ (0.298 g) was placed in a flask (50 mL), a serum cap fitted, and hydrogen passed through for ~10 min. Dichloromethane (4 mL) was then injected into the flask, and reaction was allowed to proceed for 72 h at room temperature. The flask was flushed with hydrogen at 24-h intervals. The solution, initially yellow-orange, gradually became brown-gray as the starting material disappeared and a trace of intensely colored impurity was formed. The solvent was partially evaporated in a stream of nitrogen, and methanol was added to afford $[Pt_2H_2(\mu\text{-}H)(\mu\text{-}dppm)_2][PF_6]$ (0.216 g, 74%) as a white microcrystalline solid identified by its infrared spectrum.

Reaction of $[Pt_2H(CO)(\mu\text{-}dppm)_2][PF_6]$ with Dimethylphenylphosphine. A solution of $[Pt_2H(CO)(\mu\text{-}dppm)_2][PF_6]$ (0.052 g, 0.039 mmol) in dichloromethane (0.5 mL) was prepared, under an atmosphere of carbon monoxide, in a vessel fitted with a serum cap. The carbon monoxide was replaced by helium, and complete replacement was confirmed by GLC. Dimethylphenylphosphine (0.0080 g, 0.058 mmol) in dichloromethane (0.5 mL) was added, the yellow solution darkened immediately, and effervescence occurred. Carbon monoxide was detected by GLC examination. The solution was concentrated, methanol was added, and yellow crystals of $[Pt_2H(Me_2PhP)(\mu\text{-}dppm)_2][PF_6]$ (0.036 g, 64%) were recovered by filtration and identified by their IR spectrum.[7]

Reaction of $[Pt_2H(CO)(\mu\text{-}dppm)_2][PF_6]$ with Methanethiol. Methanethiol was bubbled through a solution of $[Pt_2H(CO)(\mu\text{-}dppm)_2][PF_6]$ (0.050 g, 0.038 mmol) in dichloromethane (2 mL) for 15 min during which time the color changed from yellow-orange

to yellow. The solution was left to stand for 2 h and then was worked up by evaporation to ~0.5 mL and addition of methanol when a pale yellow precipitate of $[Pt_2H_2(\mu\text{-SMe})(\mu\text{-dppm})_2][PF_6]$ (~0.039 g, 72%) was obtained and was identified by its infrared spectrum.[8]

Reaction of $[Pt_2(CO)_2(\mu\text{-dppm})_2][PF_6]_2$ with Hydrogen. A solution of $[Pt_2(CO)_2(\mu\text{-dppm})_2][PF_6]_2$ (0.049 g, 0.033 mmol) in a mixture of dichloromethane (2 mL) and methanol (1 mL) was placed in a flask (60 mL), and the air was displaced by hydrogen at atmospheric pressure. Reaction was allowed to proceed in the dark for 5 days when carbon monoxide was shown to be present (GLC). The residue left when the solvent was completely evaporated in a stream of nitrogen and was identified as pure $[Pt_2H_2(\mu\text{-H})(\mu\text{-dppm})_2][PF_6]$ (0.044 g, 0.034 mmol) by its IR spectrum. The HPF_6, or its decomposition products, displaced in this reaction was thus shown to have volatilized with the solvent. All volatile material was therefore collected in a trap at −78 °C and was extracted with several portions of water. The aqueous extract was neutralized with alkali (0.052 mmol). Any fluorophosphate complex was hydrolyzed[20] by making the solution 1 M in HCl and heating it on a steam bath for 30 min. A PTFE vessel with a lid was used for this treatment. Finally, fluoride ion (0.063 mmol) was determined by using an "Activion" selective fluoride-sensitive electrode calibrated with samples of potassium hexafluorophosphate successfully hydrolyzed in the same way. The result shows that only approximately 32% of the expected fluoride was then recovered. The fate of the remainder is unknown. A repeat experiment gave a similar result. The fluorine content of the starting material was checked by microanalysis and found to be within 1% of the calculated value.

As a control experiment an identical solution of starting material was kept under an atmosphere of nitrogen under the same conditions. Some carbon monoxide was evolved. Examination of the IR spectrum of the residue indicated that about 25% of the dicarbonyl complex had decomposed to unidentified material.

Reaction of $[Pt_2H_2(\mu\text{-Cl})(\mu\text{-dppm})_2][PF_6]$ with Carbon Monoxide. A solution of $[Pt_2H_2(\mu\text{-Cl})(\mu\text{-dppm})_2][PF_6]$ (0.107 g, 0.080 mmol) in dichloromethane (1.5 mL) was kept in a flask (60 mL) under an atmosphere of carbon monoxide at 20 °C for 48 h. At the end of this period the presence of hydrogen was shown by GLC. Evaporation of the solvent left an orange solid identified as $[Pt_2Cl(CO)(\mu\text{-dppm})_2][PF_6]$ (0.110 g, 0.080 mmol) by its IR and ^1H NMR (60-MHz) spectra.

Attempted Reaction of $[Pt_2Cl(CO)(\mu\text{-dppm})_2][PF_6]$ with Hydrogen. Samples of this complex dissolved in dichloromethane were recovered unchanged (infrared) after being kept under an atmosphere of hydrogen for up to 72 h.

Catalysis of the Water Gas Shift Reaction. A Parr pressure reactor (300 mL) was charged with $[Pt_2H_2(\mu\text{-H})(\mu\text{-dppm})_2][PF_6]$ (0.177 g), methanol (100 mL), and water (25 mL). The vessel was then flushed with carbon monoxide, charged to a pressure of 50 psi, and then heated to 100 °C. Aliquots of gas were removed periodically for analysis for hydrogen by GC, using a 6-ft molecular sieve, 5A column. Hydrogen was formed at a constant rate [3.5 mol/(mol of catalyst)(h)] for 5 h. At the end of this period GC analysis for CO_2 was made by using a 6-ft Porapak Q column.

X-ray Structure Analysis of $[Pt_2(CO)_2(\mu\text{-dppm})_2][PF_6]_2$. Pale yellow crystals of $[Pt_2(CO)_2(dppm)_2][PF_6]_2$ were obtained from a mixture of acetone and *n*-propanol. They crack rapidly when removed from solution. Hence, the crystal selected for the diffraction measurements, of approximate dimensions 0.6 × 0.5 × 0.2 mm, was sealed in a Lindemann glass capillary together with some mother liquor.

(a) Data Collection and Reduction. The X-ray measurements were made with molybdenum radiation by using an Enraf-Nonius CAD-4F difractometer.

The unit-cell dimensions (Table II) and the orientation of the crystal mounted on diffractometer were determined by a least-squares treatment of 25 automatically centered reflections for which $12° \le \theta$ (Mo K_α) $\le 19°$. A preliminary investigation of the diffraction pattern showed that the Laue group is $2/m$, and the crystal lattice is primitive. The observed systematic absences of

Table II. Crystal Data for $[Pt_2(CO)_2(\mu\text{-dppm})_2][PF_6]_2$

a, Å	17.298 (5)[a]	empirical formula	$C_{52}H_{44}F_{12}O_2P_6Pt_2$
b, Å	18.913 (7)	fw	1504.92
c, Å	18.884 (4)	space group	$P2_1/c$
β, deg	98.63 (2)	temp, °C	20 ± 1
V, Å^3	6108	radiatn	Mo Kα (λ = 0.710 69 Å)
Z	4	monochromator	mosaic graphite crystal
d, g cm^{-3}	1.636 (calcd)	μ(Mo Kα), cm^{-1}	45.9

[a] Throughout this paper standard deviations are given in parentheses after the quantity to which they refer and are in units of the least significant digit.

reflections established that the space group is $P2_1/c$.

The intensities of 7653 hkl and $hk\bar{l}$ reflections with $3° \le \theta$ (Mo K_α) $\le 22°$ were measured by taking continuous $\theta/2\theta$ scans of 1.13° in θ. For each reflection, the integrated intensity, I, and the standard deviation, $\sigma_1(I)$, were determined from the relationships $I = C - 2(B_1 + B_2)$ and $\sigma_1(I) = [C + 4(B_1 + B_2)]^{1/2}$, where B_1 and B_2 are the counts accumulated in the first and last sixths of the scan range and C is the count accumulated in the remaining portion of the scan range. Reflections for which a preliminary scan, taken at a speed of 7°/min, gave $\sigma_1(I)/I > 1.0$ were considered weak and not examined further. Each of the other reflections was scanned either until $\sigma_1(I)/I < 0.02$ or for 75 s, whichever required less time; the scan was then repeated and the two results checked for consistency. For 46 reflections consistent results were not obtained even after two further scans. However, an examination of these reflections at the end of the structure analysis revealed none for which disagreement between $|F_o|$ and $|F_c|$ would warrant rejection from the calculations. The crystal orientation, monitored throughout the experiment, showed no change in a setting angle larger than 0.1°. The intensities of two strong reflections, remeasured every 2 h, showed no systematic variation.

The integrated intensities, I, and their standard deviations, $\sigma(I)$, where $\sigma^2(I) = \sigma_1^2(I) + (qI)^2$ and $q = 0.04$, were corrected for Lorentz and polarization effects but not for absorption. Rejection of 2128 reflections for which $I \le 3\sigma(I)$ yielded 5525 independent structure amplitudes which were used in further calculations.

(b) Structure Solution and Refinement. The positions of the platinum atoms were deduced from a Patterson function and those of the remaining non-hydrogen atoms from subsequent difference syntheses. The positional and thermal atomic parameters, the scale factor, and an empirical isotropic extinction parameter were refined by full-matrix least-squares minimization of the function $\sum w(|F_o| - |F_c|)^2$, where $w = 1/\sigma^2(|F_o|)$. The phenyl rings were constrained to $6/mmm$ symmetry and a C–C bond length of 1.395 Å. The ring carbon atoms were assigned individual isotropic and the remaining non-hydrogen atoms anisotropic thermal parameters. The contribution of the hydrogen atoms to the structure factors was accounted for but not allowed to vary; the hydrogen atoms[17] were assigned isotropic thermal parameters equal to those of the carbon atoms to which the hydrogen atoms were bonded, and their positions were calculated by assuming trigonal and tetrahedral geometries of the carbon atoms to which they are attached and a C–H bond length of 1.08 Å. The atomic scattering factors, and also the dispersion corrections for Pt and P, were taken from ref 21. At a later stage of the analysis, a difference synthesis revealed a broad region of significant electron density, well-separated from the cation and anions, that is likely to represent a highly disordered solvent molecule. The attempts to determine the geometry of this molecule were not successful.

The refinement of the structure converged at $R = 0.061$ and $R_w = 0.079$, with no parameter changing by more than 0.16σ ($R = \sum(|F_o| - |F_c|)/\sum|F_o|$ and $R_w = [\sum w(|F_o| - |F_c|)^2/\sum wF_o^2]^{1/2}$. An analysis of $\sum w(|F_o| - |F_c|)^2$ as a function of $|F_o|$, sin θ, or Miller indices revealed no obvious trends other than somewhat larger errors at lower sin θ values. In the final difference synthesis, the

(20) Van Wazer, J. R. "Phosphorus and Its Compounds"; Interscience: New York, 1958; Vol. 1, p 803.

(21) "International Tables for X-Ray Crystallography"; Kynoch Press: Birmingham, U.K., 1974; Vol. IV, Tables 2.2B and 2.3.1.

Table III. Atomic Coordinates[a] and Isotropic Thermal Parameters[b]

atom	x	y	z	U, Å²	atom	x	y	z	U, Å²
Pt(1)	30319 (3)	3596 (3)	34080 (3)		C(16)	5326 (5)	−486 (5)	2768 (5)	70 (5)
Pt(2)	17308 (3)	81 (3)	25616 (3)		C(17)	2312 (7)	30 (6)	4972 (6)	50 (4)
P(1)	3750 (2)	−80 (2)	2552 (2)		C(18)	3050 (7)	−210 (6)	5275 (6)	77 (6)
P(2)	2266 (2)	692 (2)	4274 (2)		C(19)	3120 (7)	−741 (6)	5794 (6)	93 (6)
P(3)	2353 (2)	−1007 (2)	2279 (2)		C(20)	2451 (7)	−1031 (6)	6010 (6)	81 (6)
P(4)	1196 (2)	1017 (2)	2969 (2)		C(21)	1713 (7)	−790 (6)	5707 (6)	90 (6)
P(5)	5314 (3)	2784 (3)	3904 (3)		C(22)	1643 (7)	−260 (6)	5188 (6)	78 (6)
P(6)	10126 (3)	3677 (3)	1211 (3)		C(23)	2530 (6)	1521 (4)	4733 (5)	41 (4)
F(1)	4523 (9)	2446 (11)	3615 (8)		C(24)	2127 (6)	1710 (4)	5291 (5)	57 (4)
F(2)	5339 (8)	3102 (8)	3144 (7)		C(25)	2265 (6)	2364 (4)	5627 (5)	62 (5)
F(3)	5713 (18)	2184 (15)	3725 (15)		C(26)	2805 (6)	2830 (4)	5403 (5)	70 (5)
F(4)	6092 (14)	3117 (19)	4185 (9)		C(27)	3208 (6)	2642 (4)	4844 (5)	59 (4)
F(5)	5264 (11)	2485 (12)	4663 (7)		C(28)	3070 (6)	1987 (4)	4509 (5)	52 (4)
F(6)	4823 (20)	3424 (13)	4028 (14)		C(29)	1818 (6)	−1540 (6)	1585 (6)	46 (4)
F(7)	10033 (8)	3510 (10)	2011 (7)		C(30)	1246 (6)	−1992 (6)	1776 (6)	71 (5)
F(8)	10627 (8)	2990 (7)	1190 (9)		C(31)	785 (6)	−2391 (6)	1253 (6)	94 (7)
F(9)	10215 (8)	3812 (9)	416 (7)		C(32)	396 (6)	−2339 (6)	538 (6)	102 (7)
F(10)	9621 (8)	4347 (7)	1259 (9)		C(33)	1469 (6)	−1887 (6)	347 (6)	108 (8)
F(11)	9344 (7)	3274 (7)	944 (7)		C(34)	1930 (6)	−1488 (6)	871 (6)	89 (6)
F(12)	10910 (7)	4087 (8)	1454 (7)		C(35)	2653 (6)	−1636 (5)	3000 (5)	46 (4)
O(1)	4576 (7)	722 (8)	4358 (7)		C(36)	3112 (6)	−2214 (5)	2867 (5)	63 (5)
O(2)	260 (8)	−366 (10)	1555 (10)		C(37)	3357 (6)	−2699 (5)	3411 (5)	96 (7)
C(1)	4007 (11)	592 (9)	3992 (9)		C(38)	3144 (6)	−2605 (5)	4089 (5)	79 (6)
C(2)	754 (11)	−237 (10)	1951 (10)		C(39)	2685 (6)	−2027 (5)	4222 (5)	84 (6)
C(3)	3234 (7)	−729 (8)	1937 (7)		C(40)	2440 (6)	−1543 (5)	3677 (5)	64 (5)
C(4)	1240 (8)	821 (8)	3918 (7)		C(41)	175 (4)	1145 (6)	2615 (5)	44 (4)
C(5)	4128 (6)	564 (5)	1985 (5)	44 (4)	C(42)	−44 (4)	1669 (6)	2104 (5)	67 (5)
C(6)	4270 (6)	394 (5)	1298 (5)	65 (5)	C(43)	−826 (4)	1740 (6)	1798 (5)	83 (6)
C(7)	4577 (6)	901 (5)	882 (5)	69 (5)	C(44)	−1389 (4)	1288 (6)	2003 (5)	89 (6)
C(8)	4743 (6)	1579 (5)	1153 (5)	70 (5)	C(45)	−1170 (4)	763 (6)	2514 (5)	80 (6)
C(9)	4601 (6)	1750 (5)	1841 (5)	75 (5)	C(46)	−388 (4)	692 (6)	2820 (5)	72 (5)
C(10)	4293 (6)	1243 (5)	2257 (5)	57 (4)	C(47)	1667 (6)	1851 (5)	2886 (6)	43 (4)
C(11)	4598 (5)	−551 (5)	2994 (5)	44 (4)	C(48)	1387 (6)	2448 (5)	3198 (6)	69 (5)
C(12)	4512 (5)	−988 (5)	3572 (5)	57 (4)	C(49)	1770 (6)	3095 (5)	3175 (6)	93 (6)
C(13)	5154 (5)	−1359 (5)	3924 (5)	74 (5)	C(50)	2434 (6)	3144 (5)	2840 (6)	91 (6)
C(14)	5882 (5)	−1294 (5)	3697 (5)	80 (6)	C(51)	2714 (6)	2547 (5)	2528 (6)	87 (6)
C(15)	5968 (5)	−857 (5)	3119 (5)	101 (7)	C(52)	2331 (6)	1900 (5)	2551 (6)	54 (4)

[a] Fractional coordinates have been multiplied by 10^n, $n = 5$ for Pt and 4 for other atoms. [b] The form of the isotropic temperature factor is $\exp[(-8 \times 10^{-3})\pi^2 U((\sin\theta)/\lambda)^2]$.

Table IV. Anisotropic Thermal Parameters[a]

atom	U_{11}	U_{22}	U_{33}	U_{23}	U_{13}	U_{12}
Pt(1)	462 (4)	387 (4)	311 (4)	−34 (3)	84 (3)	2 (3)
Pt(2)	484 (4)	426 (4)	345 (4)	−54 (3)	42 (3)	41 (3)
P(1)	48 (2)	44 (3)	35 (2)	−2 (2)	11 (2)	0 (2)
P(2)	50 (2)	41 (2)	34 (2)	0 (2)	9 (2)	−3 (2)
P(3)	54 (2)	42 (3)	34 (2)	−11 (2)	10 (2)	−1 (2)
P(4)	50 (2)	39 (2)	40 (2)	0 (2)	7 (2)	4 (2)
P(5)	83 (4)	84 (4)	55 (3)	11 (3)	22 (3)	−22 (3)
P(6)	76 (3)	60 (3)	83 (4)	1 (3)	22 (3)	8 (3)
F(1)	149 (13)	257 (22)	103 (11)	−16 (12)	33 (9)	−111 (14)
F(2)	159 (12)	164 (14)	82 (9)	56 (9)	19 (8)	−54 (10)
F(3)	350 (35)	264 (30)	315 (33)	129 (26)	157 (29)	223 (29)
F(4)	221 (20)	510 (46)	109 (13)	77 (20)	−6 (13)	−244 (27)
F(5)	228 (17)	305 (26)	57 (8)	58 (12)	15 (10)	−114 (17)
F(6)	495 (46)	172 (22)	261 (28)	−24 (20)	175 (30)	110 (28)
F(7)	146 (12)	223 (19)	81 (9)	0 (10)	35 (8)	22 (12)
F(8)	143 (12)	87 (10)	200 (16)	25 (10)	81 (11)	41 (9)
F(9)	133 (11)	184 (16)	89 (9)	36 (10)	20 (8)	−27 (10)
F(10)	139 (11)	68 (9)	202 (15)	−33 (10)	−10 (10)	49 (8)
F(11)	100 (9)	129 (12)	141 (12)	−47 (9)	44 (8)	−23 (8)
F(12)	104 (9)	123 (12)	138 (11)	−12 (9)	−9 (8)	−21 (8)
O(1)	59 (8)	106 (11)	80 (9)	−29 (8)	−18 (7)	−8 (7)
O(2)	72 (10)	171 (18)	155 (16)	−88 (14)	−64 (11)	28 (10)
C(1)	82 (13)	47 (11)	50 (11)	13 (9)	22 (10)	14 (9)
C(2)	68 (12)	78 (15)	54 (11)	−20 (10)	−5 (10)	12 (10)
C(3)	44 (8)	40 (9)	36 (8)	1 (7)	10 (6)	−10 (7)
C(4)	58 (9)	40 (10)	37 (8)	9 (7)	16 (7)	0 (7)

[a] The form of the anisotropic temperature factor is $\exp[(-2 \times 10^{-n})\pi^2 \Sigma_{i=1}^{3} \Sigma_{j=1}^{3} U_{ij} h_i h_j a_i^* a_j^*]$, with $n = 4$ for Pt and 3 for other atoms.

highest peaks (1.1–3.7 e Å^{-3}) were close to the positions of the Pt and C(carbonyl) atoms or were associated with the unidentified solvent molecule.

The final positional and thermal parameters of non-hydrogen atoms are presented in Tables III–IV. Coordinates of the hydrogen atoms are shown in Table V,[22] and the observed structure

amplitudes and calculated structure factors in Table OM11M100##fnt The computer programs used in this analysis are listed in ref 23.

Acknowledgment. We thank NSERC (Canada) for financial support (R.J.P.), NATO for a travel grant (R.J.P. and M.P.B.), and the University of Glasgow for a studentship (A.A.F.).

Registry No. Ia, 63911-00-2; Ib, 82864-97-9; IIa, 74587-82-9; IIb, 82864-99-1; III, 78064-41-2; IV, 69215-82-3; V, 68851-46-7; VI, 64387-54-8; VII, 81533-22-4; $[Pt_2H_2(\mu\text{-}H)(\mu\text{-}dppm)_2]Cl$, 63910-98-5; Pt, 7440-06-4; carbon monoxide, 630-08-0; hydrogen, 1333-74-0; dimethylphenylphosphine, 1486-28-8; methanethiol, 74-93-1.

Supplementary Material Available: Listings of observed and calculated structure factors (Table VI) and H atom fractional coordinates (Table V; 32 pages). Ordering information is given on any current masthead page.

(22) Supplementary material.
(23) The Enraf-Nonius Software Package for the CAD-4F diffractometer: CAD4 Data Processing Program (M. B. Hursthouse), a local version of G. M. Sheldrick's SHELX system, GEOM molecular functions program (P. R. Mallinson), and ORTEP (C. K. Johnson), adapted for the local ICL 2976 computer by P. R. Mallinson and K. W. Muir.

Comparative Reactivities of the Cyclopolyarsines $(C_6H_5As)_6$ and $(CH_3As)_5$. The Crystal and Molecular Structure of *trans*-1,2-(1,2-Diphenyldiarsino)bis[(η^5-cyclopentadienyl)dicarbonyliron], $[CpFe(CO)_2]_2(C_6H_5As)_2$

Arnold L. Rheingold,* Michael J. Foley, and Patrick J. Sullivan

Department of Chemistry, University of Delaware, Newark, Delaware 19711

Received July 1, 1982

The bis metal-substituted diarsine species $[CpFe(CO)_2]_2(C_6H_5As)_2$ (3), synthesized from $[CpFe(CO)_2]_2$ and c-$(C_6H_5As)_6$, crystallizes in the centrosymmetric monoclinic space group $P2_1/c$ [C_{2h}^5, No. 14] with a = 6.534 (2) Å, b = 11.191 (2) Å, c = 17.529 (5) Å, β = 99.60 (2) Å, V = 1263.9 (6) Å^3, and ρ = 1.73 g cm^{-3} for Z = 2 (mol wt 657.98). Diffraction data were collected with a Nicolet R3 diffractometer, and the structure was refined to R_F = 6.60% for 1579 reflections with $3° < 2\theta < 45°$ (Mo Kα radiation). The molecule is the tetrasubstituted diarsine *trans*-1,2-(1,2-diphenyldiarsino)bis[(η^5-cyclopentadienyl)dicarbonyliron]; as such it represents the first example of a new class of bridged dinuclear metal complexes. The As–Fe bond distance, 2.450 (2) Å, is long in keeping with the formal one-electron As donation to Fe. The As–As′ bond distance, 2.456 (2) Å, is within the range of "normal" As–As single bonds. In comparison, replacement of $(C_6H_5As)_6$ for $(CH_3As)_5$ in reactions with $[CpFe(CO)_2]_2$ produces as the primary Fe–As-containing product a four-membered, diiron-bridging chain $[Fe(CO)Cp]_2[\mu\text{-}catena\text{-}(CH_3As)_4]$ (4), identified by its spectroscopic properties. Accompanying the formation of 4 under open system conditions in refluxing hexane with UV irradiation is a substantial yield of $[CpFe(CO)]_4$ (~55%).

Introduction

Understanding how main-group elements bridge transition-metal centers is a major goal in inorganic chemistry. Such bridges often possess desirable structural characteristics for the design of binuclear and cluster catalysts. The extraordinary structural diversity of transition-metal carbonyl derivatives of catenated organophosphinidene and arsinidene groups (RP or RAs) makes them particularly rewarding subjects for study. Our studies of the products of the reactions of cyclopentadienylmetal carbonyls with polyorganocyclopolyarsines have shown that a characteristic feature of these reactions is ring cleavage and reformation of the resulting chain into a variety of lengths (from two to nine atoms) and configurations.[1-3]

We have also been interested in determining what effects the organic substitution on the cycloarsine precursor has in controlling the course of these reactions. West has studied the reactions of $Fe(CO)_5$ with three cyclopolyarsines: $(CH_3As)_5$, $(C_6H_5As)_6$, and $(C_6F_5As)_4$.[3-5] In the first two cases, the rings were cleaved and shortened to form $[Fe(CO)_3]_2[\mu\text{-}(RAs)_4]$ (1); with $(C_6F_5As)_4$, $[Fe(CO)_4][\eta^2\text{-}(AsC_6F_5)_2]$ (2) was obtained.

In the study we now report, we compare the reactions of $(C_6H_5As)_6$ and $(CH_3As)_5$ with $[CpFe(CO)_2]_2$. In the former case we obtain a diarsine derivative, *trans*-1,2-(1,2-diphenyldiarsino)bis(cyclopentadienyldicarbonyliron), $[CpFe(CO)_2]_2(AsC_6H_5)_2$ (3), which is the first example of a new class of arsenic-bridged dinuclear complexes. An X-ray crystallographic structure is included. In the latter case, an analogue of 1 containing a four-membered, RAs chain bridged complex is obtained: $[CpFe(CO)][\mu\text{-}(CH_3As_4)]$ (4) along with up to 55% yield of $[CpFe(CO)]_4$.

Structurally confirmed examples of complexes containing two linked RAs units are surprisingly few and are limited to three-membered heterocycles, e.g., the As_2Fe ring in 2[4] and an As_2Cr ring in $\{[Cr(CO)_5]_2(AsC_6H_5)_2\}[\mu\text{-}Cr(CO)_5]$ (5).[6]

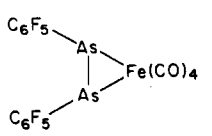

2
As–As = 2.388 (7) Å

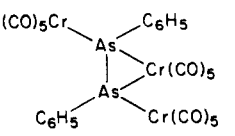

5
As–As = 2.371 Å

(1) Rheingold, A. L.; Churchill, M. R. *J. Organomet. Chem.*, in press.
(2) Rheingold, A. L.; Foley, M. J.; Sullivan, P. J. *J. Am. Chem. Soc.*, in press.
(3) Elmes, P. S.; West, B. O. *J. Organomet. Chem.* **1971**, *32*, 365.
(4) Gatehouse, B. M. *J. Chem. Soc., Chem. Commun.* **1969**, 948.
(5) Elmes, P. S.; Leverett, P.; West, B. O. *J. Chem. Soc., Chem. Commun.* **1971**, 747.
(6) Huttner, G.; Schmid, H.-G.; Frank, A.; Orama, O. *Angew. Chem.* **1976**, *88*, 255.

0276-7333/82/2301-1429$01.25/0